JIMD Reports
DOI 10.1007/8904_2011_83

RESEARCH REPORT

Alu–Alu Recombination Underlying the First Large Genomic Deletion in GlcNAc-Phosphotransferase Alpha/Beta (*GNPTAB*) Gene in a MLII Alpha/Beta Patient

Maria Francisca Coutinho · Liliana da Silva Santos · Lúcia Lacerda · Sofia Quental · Flemming Wibrand · Allan M. Lund · Klaus B. Johansen · Maria João Prata · Sandra Alves

Received: 5 May 2011 / Revised: 26 July 2011 / Accepted: 27 July 2011 / Published online: 20 October 2011

Abstract Mucolipidosis type II α/β is a severe, autosomal recessive lysosomal storage disorder, caused by a defect in the *GNPTAB* gene that codes for the α/β subunits of the GlcNAc-phosphotransferase. To date, over 100 different mutations have been identified in MLII α/β patients, but no large deletions have been reported. Here we present the first case of a large homozygous intragenic *GNPTAB* gene deletion (c.3435-386_3602 + 343del897) encompassing exon 19, identified in a ML II α/β patient. Long-range PCR and sequencing methodologies were used to refine the characterization of this rearrangement, leading to the identification of a 21 bp repetitive motif in introns 18 and 19. Further analysis revealed that both the 5′ and 3′ breakpoints were located within highly homologous *Alu* elements (*Alu-Sz* in intron 18 and *Alu-Sq2*, in intron 19), suggesting that this deletion has probably resulted from *Alu–Alu* unequal homologous recombination. RT-PCR methods were used to further evaluate the consequences of the alteration for the processing of the mutant pre mRNA *GNPTAB,* revealing the production of three abnormal transcripts: one without exon 19 (p.Lys1146_Trp1201del); another with an additional loss of exon 20 (p.Arg1145-Serfs*2), and a third in which exon 19 was substituted by a pseudoexon inclusion consisting of a 62 bp fragment from intron 18 (p.Arg1145Serfs*16). Interestingly, this 62 bp fragment corresponds to the *Alu-Sz* element integrated in intron 18.

This represents the first description of a large deletion identified in the *GNPTAB* gene and contributes to enrich the knowledge on the molecular mechanisms underlying causative mutations in ML II.

Communicated by: Verena Peters.

Competing interests: None declared.

L. da Silva Santos · S. Alves (✉)
Research and Development Unit, Department of Genetics, CGMJM, INSA, Porto Portugal
e-mail: sandra.alves@insa.min-saude.pt; alvessandra@hotmail.com

M.F. Coutinho
Research and Development Unit, Department of Genetics, CGMJM, INSA/IPATIMUP, Porto Portugal

L. Lacerda
Biochemical Genetics Unit, Department of Genetics, CGMJM, INSA, Porto Portugal

S. Quental
Quental, IPATIMUP, Porto Portugal

F. Wibrand · A.M. Lund
Department of Clinical Genetics, Rigshospitalet, Copenhagen Denmark

K.B. Johansen
Department of Pediatrics, Kolding Hospital, Kolding Denmark

M.J. Prata
IPATIMUP/ Department of Biology, Faculty of Sciences, Porto Portugal

Introduction

Mucolipidosis II α/β (ML II; MIM# 252500), ML III α/β (MIM# 252600) and ML III γ (MIM# 252605) are rare lysosomal storage diseases which share similar clinical features, including skeletal abnormalities. Among them, mucolipidosis type II α/β is clinically the most severe. The skeletal system is profoundly affected in all patients, who usually present with abnormalities in both cartilage and

bone. Linear growth decelerates during the first year of life and almost ceases during the second year. Death usually occurs between 5 and 8 years of age (Kornfeld and Sly 2001), although early death in utero as well as in the first years of life is not uncommon.

The diseases are caused by deficiencies in activity of the uridine diphosphate (UDP)-N-acetylglucosamine:lysosomal enzyme N-acetylglucosamine-1-phosphotransferase (GlcNAc-phosphotransferase), which may be reduced or absent. GlcNAc-phosphotransferase is a multimeric enzyme encoded by two genes: *GNPTAB* (α/β subunits) and *GNPTG* (γ subunit). Mutations in the *GNPTAB* gene are associated with ML II α/β and ML III α/β, whereas those in the *GNPTG* gene cause ML III γ (Raas-Rothschild et al. 2000; Tiede et al. 2004).

The *GNPTAB* gene (GenBank accession number: NG_021243.1), which codes for the α and β subunits, contains 21 exons and spans 85 kb on chromosome 12q23.3. It encodes a protein of 1,256 amino acids with a predicted molecular mass of 144 kDa (α/β precursor). Proteolytic processing of the α/β precursor generates the individual α and β subunits (Tiede et al. 2004).

To date, more than 100 different ML II α/β and ML III α/β disease-causing mutations have been identified, including 30 missense, 20 nonsense, 32 small deletions, 25 small insertions, 2 small indels, and 14 splice site mutations (Human Gene Mutation Database website [HGMD, http://www.hgmd.org] and references therein). Large genomic rearrangements were rarely reported (1.6%) including an *Alu* retrotransposition in *GNPTAB* exon 5 (Tappino et al. 2008) and the exon 2 duplication (Otomo et al. 2009), resulting from recombination between homologous regions of introns 1 and 2.

In this work, we report on a large deletion found in the *GNPTAB* gene. After performing a fine molecular screening in an ML II α/β patient, we found a homozygous genomic lesion in *GNPTAB* leading to the entire loss of exon 19 and some of its surrounding intronic regions (c.3435-386_3602 + 343del897). Analysis of the deletion breakpoints indicated that the mutation may have been generated by an unequal homologous recombination process between highly similar *Alu* elements located in two out of three regions within the gene where such kind of sequences were demonstrated to be present. Subsequent cDNA analysis revealed the presence of three abnormal transcripts created by this gross deletion at mRNA level: one without exon 19 (p.Lys1146_Trp1201del); another with an additional loss of exon 20 (p.Arg1145Serfs*2), and a third in which exon 19 was substituted by a pseudoexon inclusion consisting of a 62 bp fragment from intron 18 (p.Arg1145Serfs*16).

To the best of our knowledge, this represents the first description of a large deletion identified in the *GNPTAB* gene. Furthermore, the work adds on the knowledge of the molecular mechanisms underlying causative mutations in ML II, contributing to improved genetic counselling and prenatal diagnosis in this devastating disease.

Material and Methods

Case Description

This boy was born at 38 weeks of gestation after a caesarean section. His parents were healthy, consanguineous Palestinians who also had a healthy 3-year-old son.

Birth weight was 2,085 g, length 42 cm and head circumference 32 cm. Apgar scores were 9/1 and 10/5, but shortly after birth he developed signs of respiratory insufficiency with oxygen saturation at 70% and was treated with continuous positive airway pressure (CPAP) and oxygen.

At ultrasonography during pregnancy, the foetus was noted to have short extremities, and at birth the newborn presented with short, slightly bowed arms, and legs and a large, protruding abdomen as well as mandibular hypoplasia and gingival hyperplasia. Bilateral inguinal hernia developed at one month of age.

Initial investigations showed low phosphate at 0.8 mmol/L (reference values: 1, 4–2, 3 mmol/L), increased alkaline phosphatase at 1,518 U/L (reference values: 55–515 U/L) increasing to 1,967 U/L at age 18 days. Parathyroid hormone (PTH) was very high at 91, 2 pmol/L (reference values: 1, 1–6, 9 pmol/L). Calcium was initially slightly low, but normalised quickly without treatment. 25-hydroxy-vitamin D2 + D3 was below detection and investigations in his mother also disclosed low 25-hydroxy-vitamin D2 + D3 < 10. Thus, the initial suspicion was that the child had a severe congenital rachitis or hyperparathyroidism and X-rays were thought compatible with that (Fig. 1).

Measurement of lysosomal enzymes revealed grossly elevated hexosaminidase A and B activities in plasma, consistent with mucolipidosis type II.

The child continued to have respiratory problems and died in respiratory insufficiency at the age of 2 months.

Mutation Screening of *GNPTAB* from a gDNA Sample

Genomic DNA was isolated from fibroblasts according to standard procedures. PCR amplifications of the 21 exons and adjacent intronic regions of *GNPTAB* gene were performed using specific primers (available on request). PCR amplification was carried out using approximately 40 ng of genomic DNA, 1 × PCR reaction mix ImmoMix Red (Bioline, London, UK) and 0.25 μM of each primer.

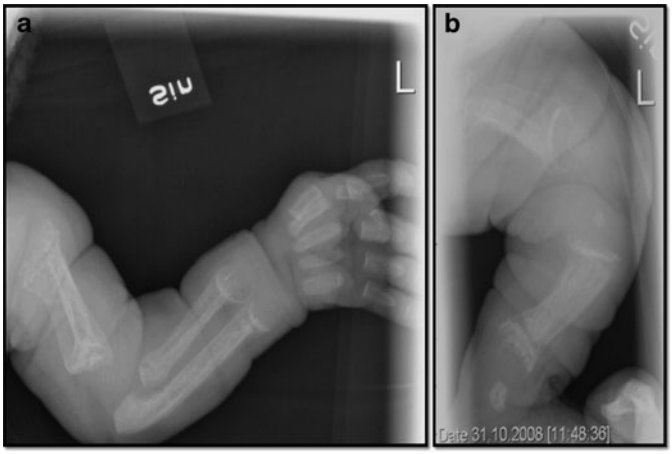

Fig. 1 *X-rays of left arm (**a**) and left leg (**b**) at birth.* In both X-rays, shortening of bones, osteopenia, and a bone-in-bone appearance are seen. The metaphyses are expanded with cupping and fraying

Thereafter, samples were heated to 95°C for 7 min, followed by 35 cycles of denaturation (30 s at 94°C), annealing (30 s at 58°C to exons 2, 3, 4, 6, 11, 12, 14, 15, 16, 17, 18, 20, and 21; 30 s at 59°C to exon 13; 30 s at 60°C to exons 1, 5, 7, 8–10, and 19) and extension (45 s at 72°C). The final extension was completed by 7 min at 72°C.

Fragments were purified with ExoSap-IT (GE Healthcare, United Kingdom) according to the manufacturer's instructions and sequenced using a BigDye Terminator Cycle Sequencing Kit (Applied Biosystems, Foster City, CA, USA) on an ABI PRISM 3130xl Genetic Analyser (Applied Biosystems, Foster City, CA, USA). Results were analysed with the sequence analysis software FINCH TV (Geospiza, Seattle, WA, USA) version 1.3.1.

Long-Range PCR and Characterization of Deletion Breakpoints

Genomic *GNPTAB* was submitted to long-range PCR using the following primers: primer forward (5′–TGGATGTTGAGTCCACTACGG–3′), designed to anneal across intron 17 and primer reverse (5′–TCATTTTCTAAAACATTCAGATGC–3′), that anneals at intron 20 (see Table 1). PCR mixture contained 500 ng of genomic DNA, 1X PCR 3.75 U Expand Long Taq-System (Roche), reaction buffer 3, 350 μM of each dNTP and 3 μM of each primer. Thereafter, the samples were heated to 94°C for 2 min, followed by 30 cycles of denaturation (10 s at 94°C), annealing (30 s at 58°C) and extension (6 min at 68°C). In the last 20 cycles, the extension time had an increment of 20 s in each one. The final extension was completed by 7 min at 68°C.

The long-range PCR fragment was purified with ExoSap-IT (GE Healthcare, United Kingdom) and sequenced. In order to detect the deletion breakpoints, several internal primers were designed to sequence introns 18 and 19 (see Table 1).

cDNA Analysis

GNPTAB cDNA analysis was performed with specific primers (see Table 1) according to the previously reported conditions (Encarnação et al. 2009).

Bioinformatic Analysis

Considering that several genomic rearrangements are frequently caused by recombination events promoted by repetitive elements present in the human genome, the DNA sequences flanking the 5′ and 3′ deletion breakpoints were screened for the presence of such elements with the RepeatMasker software (http://repeatmasker.org).

The scores for the splice site junctions were obtained with the Maxent programme (http://genes.mit.edu/burgelab/maxent/Xmaxentscanscoreseqacc.html) (Yeo and Burge 2004). Ideal Maxent splice site scores are: 11.81 (5′ss) and 13.59 (3′ss).

Mutation Nomenclature

As reference for the *GNPTAB* gene, we used the sequence available at http://www.ncbi.nlm.nih.gov/nuccore/NG_021243.1 (GenBank accession number: NG_021243.1).

As reference for the *GNPTAB* mRNA, we used the sequence available at http://www.ncbi.nlm.nih.gov/nuccore/NM_024312.4 (GenBank accession number: NM_024312.4).

Table 1 Complete list of primers used to perform this work

gDNA amplification of exon 19 and its intronic boundaries

	Localization	Sequence	Annealing temperature	PCR product size	Reference
Forward	Intron 18	5′-CCCATAGCTAAAAGGCCATCTACC-3′	60°C	436 bp	Encarnação et al. (2009)
Reverse	Intron 19	5′-GTATACACTCACCCACACACATGC-3′			Encarnação et al. (2009)
Forward 2	Intron 18	5′-TTTGGAATCCACATCCTTGTT-3′	60°C	391 bp	This study
Reverse 2	Intron 19	5′-TGGGCAACAAGAACAAAACTC-3′			This study

gDNA long range PCR

	Localization	Sequence	Annealing temperature	PCR product size	Reference
Forward	Intron 17	5′–TGGATGTTGAGTCCACTACGG–3′	58°C	8,392 bp	This study
Reverse	Intron 20	5′–TCATTTTCTAAAACATTCAGATGC–3′			This study

Optimised sequencing of the long range amplicon

	Localization	Sequence	Annealing temperature	PCR product size	Reference
Forward 1	Intron 18	5′–TGGGCTCAAGCAATCCTCC–3′	Not applicable		This study
Forward 2	Intron 18	5′–CCAGGTTTAGAGAAAGATGAA–3′			This study
Forward 3	Intron 18	5′–TTTTGGCGAATCTACTTCAAAAG–3′	Not applicable		This study
Forward 4	Intron 18	5′–CCACATCTGGCTAATTTTCATA–3′			This study
Reverse 1	Intron 19	5′–AGGCGAGAGGGTATGAACTG–3′	Not applicable		This study
Reverse 2	Intron 19	5′–TAGCAGCAATATTCATCCTAAT–3′			This study
Reverse 3	Intron 19	5′–CAATATTGCTAGTGATTATTCCCACA–3′	Not applicable		This study
Reverse 4	Intron 19	5′–CAGTTGAATAAATGAAGTTCC–3′			This study

cDNA amplification of a fragment ranging from exons 17–21

	Localization	Sequence	Annealing temperature	PCR product size	Reference
Forward	Exon 17	5′-CCAGTAACTGACAAAATCCA-3′	55°C	734 bp	Encarnação et al. (2009)
Reverse	Exon 21	5′-ACAGGTCCATGAGCAAATTC-3′			Encarnação et al. (2009)

Results and Discussion

The molecular examination of a ML II patient was initially assessed through routine procedures, which involved amplification and direct sequencing of *GNPTAB* exons and flanking intronic regions (Encarnação et al. 2009). However, the failure to amplify the fragment correspondent to exon 19 and its intronic boundaries from the patient's DNA in face of normal amplification from control DNA, led us to suspect that a large deletion could underlie the molecular defect. To exclude that the nonamplification of the fragment containing exon 19 was due to any polymorphic variation in the primer's annealing region, a second pair of primers was used that again resulted in unsuccessful amplification of exon 19 (see primer sequences in Table 1). No mutations were found in the remaining regions sequenced.

To investigate whether a large deletion was indeed involved, a long-range PCR was designed to amplify *GNPTAB* genomic DNA encompassing exons 18–20 and respective intronic flanking sequences. This approach resulted in amplification of different-sized fragments in the patient and controls. The electrophoretic pattern in 2% agarose gel of the long-PCR products clearly indicated that the amplified fragment in the patient was shorter (approximately 7,000 bp) than the expected size (8,392 bp) of the control (data not shown). To detect the deletion junction region and disclose the exact size of the gene loss, four internal primers annealing in intron 18 and another four annealing in intron 19 were used for optimal sequencing of the amplicon obtained through long-range PCR (Table 1).

The sequencing results allowed the identification of the deletion breakpoints and the determination of the deletion

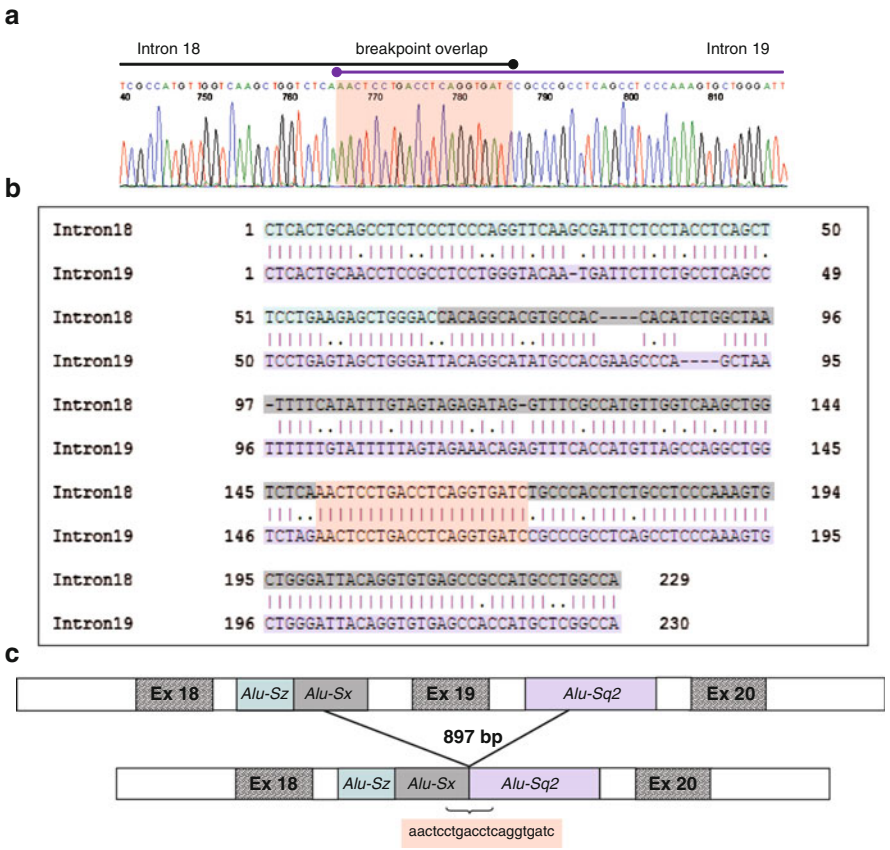

Fig. 2 *Characterization of the deletion breakpoints.* (**a**) Electropherogram evidencing the junction fragment resulting from the large deletion in the affected individual. Partial representation of introns 18 and 19 with the 21 bp breakpoint overlap highlighted in *pink*. (**b**) Nucleotide sequence alignment of the genomic sequence from introns 18 and 19 of the *GNPTAB* gene. Sequence gaps are indicated by *dashed lines*, *short vertical lines* indicate matched bases between both introns. Sequence highlighted in *aquamarine* corresponds to the *Alu-Sz* element of intron 18; sequence highlighted in *grey* corresponds to the *Alu-Sx* element of the same intron and, finally, the one highlighted in *light violet*, indicates the *Alu-Sq2* element of intron 19. (**c**) Schematic representation of the deletion breakpoints and their flanking *Alu* elements. C1 represents a normal gDNA fragment and C2 schematizes the mutated gDNA with a deletion of 897 bp including the last 386 nucleotides of intron 18, exon 19 (168 bp), and the first 343 bp of intron 19

extension which was 897 bp and included the last 386 nucleotides of intron 18, exon 19 (168 bp), and the first 343 bp of intron 19 (c.3435-386_3602 + 343del897). Furthermore, we verified that a 21 bp perfect sequence overlap ("aactcctgacctcaggtgatc"; Fig. 2a, b) occurred at the two deletion breakpoints: the same sequence stretch was present in intron 18 and intron 19. Additional sequence analysis revealed that, in both introns, the "aactcctgacctcaggtgatc" motif was flanked by highly homologous sequences (Fig. 2b). The sequence alignment of the genomic regions (introns 18 and 19), surrounding the 21 bp overlapping segment, showed high homology: in particular, the 149 nucleotides upstream and the 59 nucleotides downstream of the deletion breakpoints shared 76.5% and 89.8% homology, respectively. Since this high level of sequence homology suggested the presence of *Alu* elements, both full-length intron sequences were submitted to analysis by the Repeat Masker Web Server to search for interspersed repeat elements. The "in silico" analysis revealed that two next *Alu* sequences (*Alu-Sz* followed by *Alu-Sx*) were present in intron 18 and another (*Alu Sq2*) in intron 19. It was therefore evident that both the 5′ and 3′ breakpoints of the deletion were located within highly homologous Alu elements (Fig. 2c). Additionally, when the "in silico" analysis was extended to the entire gene, we observed that the 3′UTR region not only was highly homology to introns 18 and 19 but also showed an Alu element (*Alu-Sx* family) bearing the motif "aactcctgacctcaggtgatc" (data not shown).

Alu elements are short interspersed elements (SINEs), normally located within introns, and 3′ untranslated regions of genes, which are considered mutational "hotspots" for large gene rearrangements.

Thus, it is highly probable that the mutation here detected has arisen after an *Alu–Alu* unequal recombination event. During DNA replication, the primer and template strands might have transiently dissociated and then reassociated in a misaligned configuration mediated by the

"aactcctgacctcaggtgatc" sequences within introns 18 and 19, generating the large deletion (Fig. 2c).

The mechanism involving unequal homologous recombination between highly similar *Alu* elements has been described as contributing to several genetic diseases (Deininger and Batzer 1999), such as ornithine transcarbamylase deficiency (OTCD) (Quental et al. 2009), Von Hippel-Lindau disease (VHL) (Franke et al. 2009), Kindler syndrome (Has et al. 2006) and maple syrup urine disease (Quental et al. 2008).

This distribution of *Alu* sequences within *GNPTAB,* indicates that homologous recombination events mediated by similar *Alu* elements might involve introns 18 and 19 and the 3′UTR, increasing the risk of generating gross defective alleles at the gene, some of which may remain unidentified. We can hypothesise that at least some ML II patients from whom no RNA samples were available and, in whom only one mutant allele has previously been found (Encarnação et al. 2009; Tappino et al. 2009; Otomo et al. 2009; Zarghooni and Dittakavi 2009), might be compound heterozygous for large deletions caused by *Alu*-mediated mechanisms. The confirmation of that status would be of obvious implications in genetic counselling and prenatal diagnosis, but in which regards to the partially characterised patients from our series (Encarnação et al. 2009), RNA samples were available for testing and no gross deletions were found in either of them. Another important point that deserves attention is the fact that patients who have already been classified as homozygous for other *GNPTAB* mutations may be misclassified if that mutation happens to occur in a region where one of the alleles carries a gross deletion. Such may be of great importance for a correct establishment of genotype–phenotype correlations.

Finally, to address the impact of the novel deletion upon RNA processing, RT_PCR of the *GNPTAB* cDNA region encompassing exons 17–21 (734 bp) revealed the presence of three abnormal transcripts (Fig. 3a): one without exons 19 and 20 (Fig. 3b); transcript 1; another with the loss of exon 19 alone (Fig. 3b; transcript 2), and a third in which exon 19 was substituted by a pseudoexon inclusion consisting of a 62 bp fragment from intron 18 (Fig. 3b; transcript 3). At a protein level, all three transcripts give rise to aberrant truncated proteins: transcript 1 (Fig. 3) leads to the substitution of an arginine by a serine at position 1145, with a consequent frameshift that results in the introduction of a novel amino acid at position 1146 and of a PTC at position 1147 (p.Arg1145Serfs*2); transcript 2 leads to the formation of a mutant protein with less 56 amino acids between positions 1146 and 1201 (p.Lys1146_Trp1201del); transcript 3 (Fig. 3) also leads to

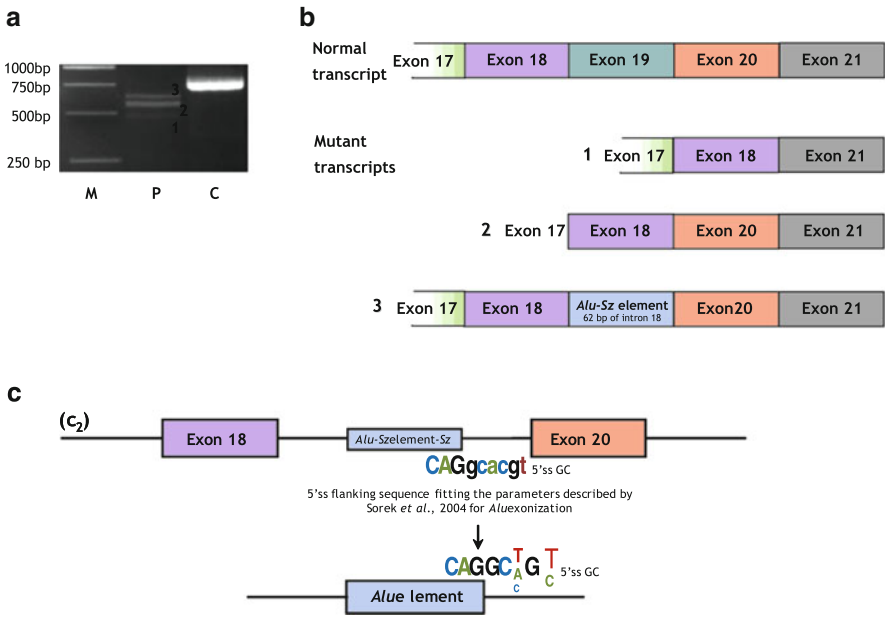

Fig. 3 *Agarose gel showing the GNPTAB transcripts observed in the affected individual together with schematic views of each transcript's constitution.* (**a**) Agarose gel showing the *GNPTAB* transcripts observed in the affected individual. *P* patient, *C* control, *M* marker (GeneRuller™ DNA Ladder 100–10,000 bp, Fermentas). (**b**) Schematic representation of the three abnormal transcripts. The first transcript presented loss of exons 19 and 20 (**b1**). The second transcript presented the loss of exon 19 alone (**b2**) and the third one instead of exon 19 had an inclusion of 62 bp of the *Alu-Sz* element of intron 18 (**b3**). (**c**) Schematic representation of the potential 5′ss of the pseudoexon showing its correspondence to one of the sequences referred to by Sorek et al. (2004) as necessary for the creation of alternatively spliced *Alu* exons

a frameshift after the substitution Arg1145Ser with introduction of 15 novel amino acids followed by a PTC (p.Arg1145Serfs*16).

The finding that this 62 bp fragment corresponded to the majority of the *Alu-Sz* element integrated in intron 18 (Fig. 3c), is quite curious since there are several recent studies in which pseudoexons were characterised as *Alu* or LINE elements (Knebelmann et al. 1995; Meili et al. 2009; Mitchell et al. 1991; Pérez et al. 2009; Vervoort et al. 1998), as well as with recent estimates indicating that up to 5% of human alternative exons could be derived from *Alu* sequences (Sorek et al. 2004; Tazi et al. 2009; Wood et al. 2007). With this in mind, we looked for *Alu* sequences within *GNPTAB* exons, but no repetitive sequences were found in any of them, indicating that exonization was not an evolutionary mechanism at the *GNPTAB* gene. According to the current state of knowledge, exonization of *Alu* sequences depends almost solely on the sequence composition of the potential 3′ and 5′ splice sites. *Alus* containing the 3′ss sequences described by Lev-Maor et al. (2003) or the 5′ss sequences reported by Sorek et al. (2004), are highly scored to become alternatively spliced exons. On these grounds, after analysing within intron 18 the flanking sequences of both potential splice sites of the *Alu-Sz* element, we verified that although the 3′ss sequence was different from that described by Lev-Maor et al. (2003), the residues of intron 18 that are flanking the potential 5′ss corresponded to one of the sequences referred to by Sorek et al. (2004) as necessary for the creation of alternatively spliced *Alu* exons (Fig. 3c). Consistently, the MaxEnt prediction of scores for the splice site junctions pointed towards an activation of a downstream cryptic splice site in intron 18 (5′ss = 9.70) to produce the transcript with the pseudoexon inclusion (Fig. 3b; transcript 3). Taking this data into account, it seems that the novel deletion c.3435-386_3602 + 343del897, here reported activates a cryptical splice site on the *Alu-Sz* element in such a way that it is recognised as an exon.

Altogether, these results clearly demonstrate that this deletion causes a serious aberration in the splicing pattern of the mutant pre mRNA *GNPTAB*, with three mutant transcripts being formed and at the protein level, which would have gone unnoticed if only simple gDNA analyses had been carried out.

Conclusion

In this study, we present the first report of a large deletion in the *GNPTAB* gene (c.3435-386_3602 + 343del897). The mutation was found in a severely affected ML II patient with prenatal onset, severe skeletal changes and hyperparathyroidism and causes homozygous loss of exon 19 and some of its surrounding intronic regions. Given the presence of two highly homologous *Alu* elements in exons 18 and 19, the deletion was probably caused by a process of unequal homologous recombination. Processing of the mutant pre mRNA *GNPTAB* causes production of three abnormal transcripts: one without exon 19 (p.Lys1146_Trp1201del); another with an additional loss of exon 20 (p.Arg1145-Serfs*2) and a third in which exon 19 was substituted by a pseudoexon inclusion consisting of a 62 bp fragment from intron 18 (p.Arg1145Serfs*16). It is important to take into account the possible existence of such large deletions when performing molecular screenings of the *GNPTAB* gene, being aware that when present in heterozygosity, they might easily escape detection through DNA genomic analyses. Without direct cDNA examination, this kind of mutation can remain unidentified.

From the results obtained, we recommend that ML II α/β and ML III α/β cases with only one mutant allele detected at direct sequencing should be further examined for the presence of large heterozygous deletions to strengthen the accuracy of genetic counselling and prenatal diagnosis in the families at risk.

Acknowledgments This work was supported by FCT - project PIC/IC/83252/2007 (http://alfa.fct.mctes.pt/). Coutinho MF and Quental S received grants from the FCT (SFRH/BD/48103/2008; SFRH/BPD/64025/2009).

One Sentence Take-Home Message

First large genomic deletion in the *GNPTAB* gene.

References

Deininger PL, Batzer MA (1999) Alu repeats and human disease. Mol Genet Metab 67:183–93

Encarnação M, Lacerda L, Costa R et al (2009) Molecular analysis of the *GNPTAB* and *GNPTG* genes in 13 patients with mucolipidosis type II or type III - identification of eight novel mutations. Clin Genet 76:76–84

Franke G, Bausch B, Hoffmann MM et al (2009) Alu-Alu recombination underlies the vast majority of large VHL germline deletions: molecular characterization and genotype-phenotype correlations in VHL patients. Hum Mutat 30:776–86

Has C, Wessagowit V, Pascucci M et al (2006) Molecular basis of Kindler syndrome in Italy: novel and recurrent Alu/Alu recombination, splice site, nonsense, and frameshift mutations in the KIND1 gene. J Invest Dermatol 126:1776–83

Knebelmann B, Forestier L, Drouot L et al (1995) Splice-mediated insertion of an Alu sequence in the COL4A3 mRNA causing autosomal recessive Alport syndrome. Hum Mol Genet 4:675–9

Kornfeld S, Sly WS (2001) I-cell disease and pseudo-Hurler polydystrophy: disorders of lysosomal enzyme phosphorylation and localisation. In: Scriver CR, Beaudet AL, Sly WS, Valle D (eds) The metabolic and molecular bases of inherited disease, 8th edn. McGraw-Hill, New York, pp 3421–42

Lev-Maor G, Sorek R, Shomron N et al (2003) The birth of an alternatively spliced exon: 3′ splice-site selection in Alu exons. Science 300:1288–91

Meili D, Kralovicova J, Zagalak J et al (2009) Disease-causing mutations improving the branch site and polypyrimidine tract: pseudoexon activation of LINE-2 and antisense Alu lacking the poly(T)-tail. Hum Mutat 30:823–31

Mitchell GA, Labuda D, Fontaine G et al (1991) Splice-mediated insertion of an Alu sequence inactivates ornithine delta-amino-transferase: a role for Alu elements in human mutation. Proc Natl Acad Sci 88:815–9

Otomo T, Muramatsu T, Yorifuji T et al (2009) Mucolipidosis II and III alpha/beta: mutation analysis of 40 Japanese patients showed genotype-phenotype correlation. J Hum Genet 54:145–51

Pérez B, Rincón A, Jorge-Finnigan A et al (2009) Pseudoexon exclusion by antisense therapy in methylmalonic aciduria (MMAuria). Hum Mutat 30:1676–82

Quental R, Azevedo L, Rubio V et al (2009) Molecular mechanisms underlying large genomic deletions in ornithine transcarbamylase (OTC) gene. Clin Genet 75:457–64

Quental S, Martins E, Vilarinho L et al (2008) Maple syrup urine disease due to a new large deletion at BCKDHA caused by non-homologous recombination. J Inherit Metab Dis 20(4):463–472

Raas-Rothschild A, Cormier-Daire V, Bao M et al (2000) Molecular basis of variant pseudo-hurler polydystrophy (mucolipidosis IIIC). J Clin Invest 105:673–681

Sorek R, Lev-Maor G, Reznik M et al (2004) Minimal conditions for exonization of intronic sequences: 5′ splice site formation in alu exons. Mol Cell 14:221–31

Tappino B, Chuzhanova NA, Regis S et al (2009) Molecular characterization of 22 novel UDP-N-acetylglucosamine-1-phosphate transferase alpha- and beta-subunit (GNPTAB) gene mutations causing mucolipidosis types IIalpha/beta and IIIalpha/beta in 46 patients. Hum Mutat 30:E956–E973

Tappino B, Regis S, Corsolini F et al (2008) An *Alu* insertion in compound heterozygosity with a microduplication in GNPTAB gene underlies Mucolipidosis II. Mol Genet Metab 93:129–33

Tazi J, Bakkour N, Stamm S (2009) Alternative splicing and disease. Biochim Biophys Acta 1792:14–26

Tiede S, Cantz M, Raas-Rothschild A et al (2004) A novel mutation in UDP-N-acetylglucosamine-1-phosphotransferase gamma subunit (GNPTAG) in two siblings with mucolipidosis type III alters a used glycosylation site. Hum Mutat 24:535–536

Vervoort R, Gitzelmann R, Lissens W et al (1998) A mutation (IVS8 + 0.6kbdelTC) creating a new donor splice site activates a cryptic exon in an Alu-element in intron 8 of the human beta-glucuronidase gene. Hum Genet 103:686–93

Wood M, Yin H, McClorey G (2007) Modulating the expression of disease genes with RNA-based therapy. PLoS Genet 3:e109

Yeo G, Burge CB (2004) Maximum entropy modeling of short sequence motifs with applications to RNA splicing signals. J Comput Biol 11:377–394

Zarghooni M, Dittakavi SS (2009) Molecular analysis of cell lines from patients with mucolipidosis II and mucolipidosis III. Am J Med Genet 149A:2753–61